

The PB2-E627K Mutation Attenuates Viruses Containing the 2009 H1N1 Influenza Pandemic Polymerase

Brett W. Jagger,^{a*} Matthew J. Memoli,^a Zong-Mei Sheng,^a Li Qi,^a Rachel J. Hrabal,^a Genevieve L. Allen,^a Vivien G. Dugan,^a Ruixue Wang,^a Paul Digard,^b John C. Kash,^a and Jeffery K. Taubenberger^a

Viral Pathogenesis and Evolution Section, Laboratory of Infectious Diseases, National Institute of Allergy and Infectious Diseases, National Institutes of Health, Bethesda, Maryland, USA,^a and Division of Virology, Department of Pathology, Cambridge University, Cambridge, United Kingdom^b

* Present address: Division of Virology, Department of Pathology, Cambridge University, Cambridge, United Kingdom.

ABSTRACT The swine-origin H1N1 influenza A virus emerged in early 2009 and caused the first influenza pandemic in 41 years. The virus has spread efficiently to both the Northern and the Southern Hemispheres and has been associated with over 16,000 deaths. Given the virus's recent zoonotic origin, there is concern that the virus could acquire signature mutations associated with the enhanced pathogenicity of previous pandemic viruses or H5N1 viruses with pandemic potential. We tested the hypothesis that mutations in the polymerase PB2 gene at residues 627 and 701 would enhance virulence but found that influenza viruses containing these mutations in the context of the pandemic virus polymerase complex are attenuated in cell culture and mice.

IMPORTANCE Influenza A virus (IAV) evolution is characterized by host-specific lineages, and IAVs derived in whole or in part from animal reservoirs have caused pandemics in humans. Because IAVs are known to acquire host-adaptive genome mutations, and since the PB2 gene of the 2009 H1N1 virus is of recent avian derivation, there exists concern that the pathogenicity of the 2009 H1N1 influenza A pandemic virus could be potentiated by acquisition of the host-adaptive PB2-E627K or -D701N mutations, which have been shown to enhance the virulence of other influenza viruses. We present data from a mouse model of influenza infection showing that such mutations do not increase the virulence of viruses containing the 2009 H1N1 viral polymerase.

Received 3 March 2010 Accepted 8 March 2010 Published 18 May 2010

Citation Jagger, B. W., M. J. Memoli, Z.-M. Sheng, L. Qi, R. J. Hrabal, et al. 2010. The PB2-E627K mutation attenuates viruses containing the 2009 H1N1 influenza pandemic polymerase. *mBio* 1(1):e00067-10. doi:10.1128/mBio.00067-10.

Editor W. Ian Lipkin, Columbia University

Copyright © 2010 Jagger et al. This is an open-access article distributed under the terms of the Creative Commons Attribution-Noncommercial-Share Alike 3.0 Unported License, which permits unrestricted noncommercial use, distribution, and reproduction in any medium, provided the author and source are credited.

Address correspondence to Jeffery K. Taubenberger, taubenbergerj@niaid.nih.gov.

Influenza A viruses (IAVs) cause significant human respiratory disease in the form of annual, epidemic recurrences and the sporadic emergence of novel viruses that may give rise to pandemics (1). In April 2009, a novel swine-origin H1N1 influenza A virus was identified from patients in Mexico and the United States (2), spread globally (3), and caused the first influenza pandemic since 1968 (4). Influenza pandemics vary greatly in their severity, as measured by the numbers of pneumonia and influenza deaths they cause (5). While the pandemic's full impact cannot yet be assessed, as of 21 February 2010 there have been at least 16,226 deaths and millions of cases worldwide (6). The worst influenza pandemic on record was the 1918-1919 "Spanish" influenza, which killed approximately 50 million people globally (7). It has been hypothesized that the 1918 pandemic circulated in a less virulent form in an initial spring-summer wave and a more virulent form in a second major wave (8). There has been speculation that the 2009 pandemic could also develop enhanced virulence following further adaptation to the human host, but data in support of these hypotheses are limiting (9).

The basis for enhanced pathogenicity of pandemic influenza viruses relates in part to antigenic novelty and the lack of protective immunity in all or parts of the population but also likely relates to inherent viral virulence factors that differ between virus strains. Pandemic viruses, derived at least in part from zoonotic

infections, must also be sufficiently host adapted to efficiently replicate and transmit in humans (10). The molecular basis as to why the 1918 pandemic virus, especially in the fall and winter of 1918-1919 (11), had enhanced pathogenicity is polygenic and still not fully elucidated. Experimental animal models have shown that the genes encoding the surface proteins hemagglutinin (HA) and neuraminidase (NA) and the genes encoding the viral ribonucleoprotein polymerase (RNP) complex (consisting of the viral polymerase subunits PB2, PB1, PA, and nucleoprotein [NP]) contain still-undefined virulence factors (12-16). Similarly, the Asian lineage of highly pathogenic avian influenza (HPAI) virus H5N1 has caused very high mortality rates among those humans with clinically apparent infections (286 deaths out of 478 confirmed cases since 2003 [17]), but sustained human-to-human transmission has not been observed.

Mutations in the genes encoding the influenza A viral RNP have been implicated in the adaptation of avian influenza viruses to humans (18, 19). The PB2 subunit (20), in particular, PB2 residue 627 (PB2-627), has been identified as an important determinant of host range restriction (21) and virulence in animal models (22, 23). Avian influenza viruses generally encode a glutamic acid at this site, while human isolates typically encode a lysine. Residue 701, residing in a region of PB2 implicated in nuclear localization (24, 25), has similarly been identified as a host-adaptive locus (26),

TABLE 1 Characteristics of viruses evaluated in this study

Name	Genotype	Nadir wt (% of baseline)	Lung titer (PFU/g)		Histopathology
			3 dpi	5 dpi	
rNY312	NY312	-0.62	2.6×10^3	2.7×10^3	Few inflammatory foci; very rare viral antigen
rNY312-K627E	NY312, PB2-K627E	-0.57	4.1×10^3	3.5×10^3	Few inflammatory foci; very rare viral antigen
1918RNP	1918RNP:NY312	-15.9	7.7×10^5	6.5×10^5	Moderate-marked necrotizing bronchiolitis; abundant bronchiolar viral antigen
1918RNP-K627E	1918RNP, PB2-K627E:NY312	+0.54	4.4×10^4	2.6×10^5	Few inflammatory foci; minimal bronchiolar viral antigen
VN1203RNP	VN1203RNP:NY312	-15.7	4.2×10^5	2.6×10^3	Moderate-marked necrotizing bronchiolitis; abundant bronchiolar viral antigen
S09RNP	S09RNP:NY312	-4.93	5.2×10^4	1.4×10^2	Focal alveolitis; predominantly alveolar viral antigen
S09RNP-E627K	S09RNP, PB2-E627K:NY312	-8.06	9.9×10^5	2.3×10^5	Mild bronchiolitis; moderate bronchiolar viral antigen
CA09RNP	CA09RNP:NY312	-4.18	2.2×10^5	4.1×10^4	Mild, focal necrotizing bronchiolitis; low levels of bronchiolar viral antigen
CA09RNP-E627K	CA09RNP, PB2-E627K:NY312	-0.83	1.1×10^3	4.3×10^2	Few inflammatory foci; very rare viral antigen
CA09RNP-D701N	CA09RNP, PB2-D701N:NY312	-1.71	1.2×10^4	2.5×10^3	Few inflammatory foci; very rare viral antigen

with the D701N mutation increasing both replication in mice (27, 28) and transmission in guinea pigs (29). Independent examples of selection of the PB2-D701N mutation have also been observed, for example, in the nonpandemic avian origin European swine H1N1 viruses (30) as well as in some HPAI H5N1 viruses.

Along with its established role in host adaptation, the influenza A RNP has also been noted as a key determinant of virulence. A virus containing the 1918 RNP on the background of a seasonal human H1N1 virus was found to increase viral replication and worsen histopathologic findings in the lower respiratory tract in ferrets (16). Likewise, a reassortant virus containing the polymerase genes (encoding PB2, PB1, and PA) of the highly pathogenic H5N1 isolate A/Vietnam/1203/2004 (referred to as VN1203), isolated from a fatal human infection, and the nonpolymerase genes of A/chicken/Vietnam/C58/04 (H5N1) (referred to as CH58), an HPAI isolate that is nonlethal in mice and ferrets, retained significant lethality in these animals. In contrast, a virus containing the polymerase genes of CH58 and the nonpolymerase genes of VN1203 was entirely nonlethal even though both viruses express an HA with a polybasic cleavage site insertion (31), the principal determinant of high pathogenicity in poultry infections (32).

The 2009 pandemic H1N1 virus possesses a PB2 protein of relatively recent avian derivation, and this protein retains the avian consensus residues PB2-627E and -701D. There has been concern that the 2009 pandemic H1N1 virus could acquire human-adaptive changes at these residues (33), and two viral isolates with the PB2-E627K mutation have been reported (34). It is therefore critical to assess the likelihood that pandemic H1N1 viruses with such mutations would have increased virulence.

RESULTS

To evaluate replicative properties and virulence factors specifically attributable to the RNP complex of the 2009 pandemic H1N1 virus, we generated a reassortant virus containing the four RNP genes (encoding PB1, PB2, PA, and NP) of a representative isolate, A/California/04/2009 (H1N1) (referred to as CA09), on the back-

ground of the remaining four gene segments—encoding the hemagglutinin (HA), neuraminidase (NA), matrix (M), and nonstructural (NS) proteins—from a recent seasonal human influenza virus, A/New York/312/2001 (H1N1) (referred to as NY312) (15); we term the reassortant virus CA09RNP. Isogenic chimeric viruses were chosen to control for differences in HA that could affect cellular tropism and pathogenicity *in vivo*. As positive controls of RNP-attributable virulence, viruses containing the RNPs of the 1918 pandemic (1918RNP) and VN1203 (VN1203RNP) viruses were also constructed on the NY312 background. To assess the impact of the PB2-E627K change on an RNP of nonmammalian-adapted, avian origin, we generated a virus with the appropriate segments from the low-pathogenicity avian virus A/green-winged teal/Ohio/175/1986 (H2N1) on the NY312 background, termed S09RNP. As a further control, the parental NY312 virus (rNY312) was also rescued. Characteristics of the viruses evaluated in this study are shown in Table 1.

To test the hypothesis that introduction of PB2 mutations at residue 627 or 701 into the RNP of the 2009 pandemic H1N1 virus would enhance virulence, we evaluated replication kinetics and pathogenicity. First, we observed the growth of rescued viruses in cell culture. All rescued viruses propagated well in MDCK cells (data not shown). To characterize the chimeric viruses in cells of human origin, replication kinetics in the A549 lung cell line were assessed (Fig. 1). As expected, the 1918RNP virus grew to a significantly higher (>1 log) mean peak titer than the control rNY312 virus ($P = 0.0083$). The CA09RNP virus grew to high titers similar to those of the 1918RNP virus ($P = 0.0088$ for comparison to rNY312), as did the VN1203RNP virus ($P = 0.019$ for comparison to rNY312), but the low-pathogenicity avian RNP genes (S09RNP virus) did not show significantly enhanced growth compared to the NY312 parent ($P = 0.050$) (Fig. 1). To determine the impact of host-adaptive mutations on replication, further selected isogenic pairs of viruses in which PB2 residue 627 or 701 was mutated to the mammalian or avian consensus residue as appropriate were then created. A 1918RNP virus in which PB2 residue 627 was

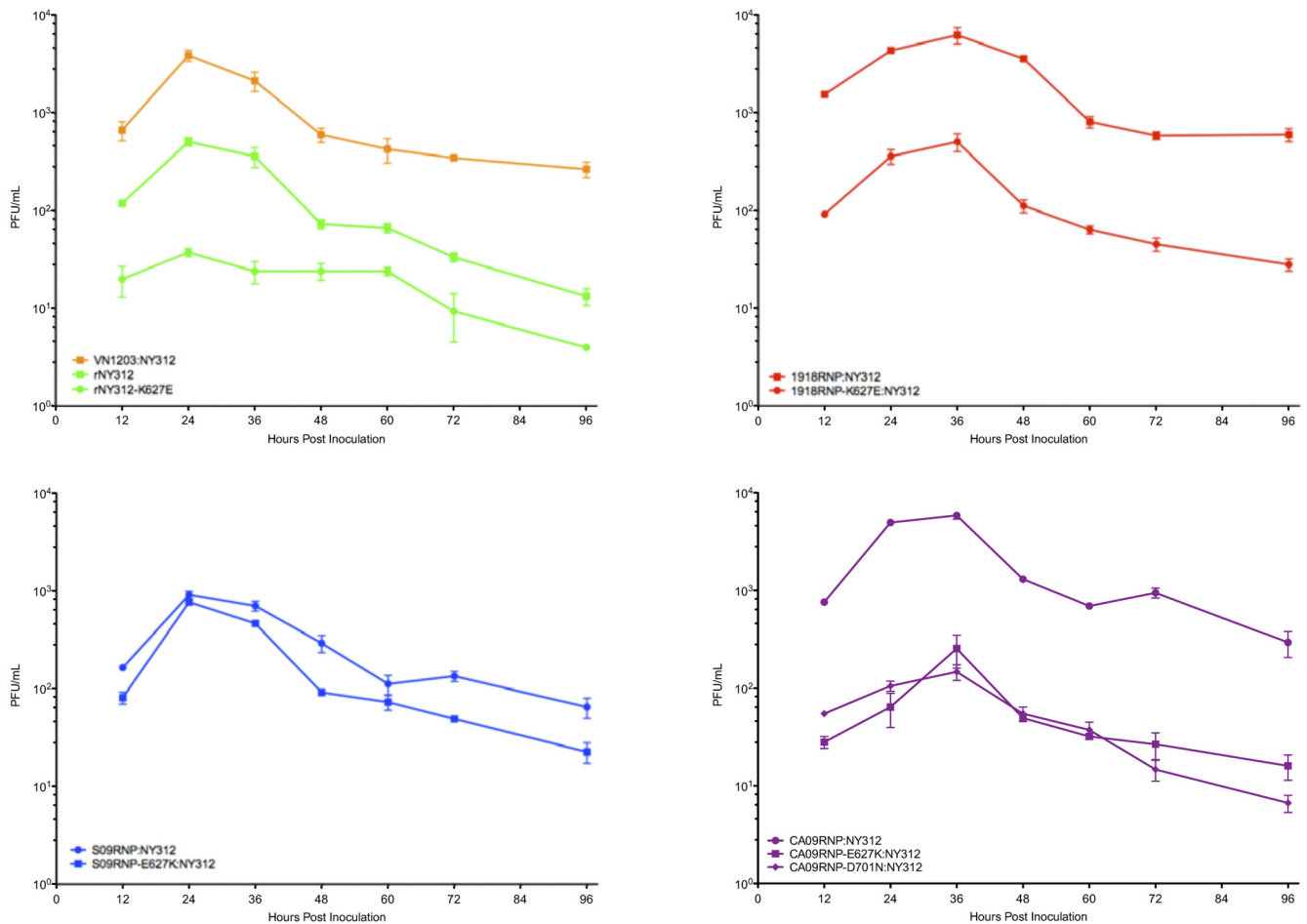


FIG 1 Viral replication kinetics in A549 cells at 37°C. Cells were infected at a 0.01 multiplicity of infection. Supernatants from infected A549 cells were collected at 12-h intervals, and viral titer was determined by a plaque assay. Cultures and measurements were performed in triplicate. Titers are expressed as numbers of PFU per milliliter. Error bars represent standard errors of the means (SEM). See the key for the different viruses evaluated.

“back-adapted” to the avian glutamic acid (1918RNP-K627E) consistently grew to a 1- to 2-log-lower peak titer ($P = 0.042$) than the 1918RNP virus. Conversely, mutation of PB2 residue 627 in the avian RNP S09RNP virus to the mammalian consensus residue (S09RNP-E627K) had little effect on growth in A549 cells. Next, the impact of the PB2-E627K (CA09RNP-E627K) and D701N (CA09RNP-D701N) mutations on viruses containing the 2009 pandemic RNP was assessed. Surprisingly, rather than increasing the growth of the CA09RNP virus, both of these mutant viruses grew to a 1- to 2-log-lower peak titer than the parental CA09RNP virus ($P = 0.0058$ and 0.0075 , respectively).

To evaluate pathogenicity *in vivo*, the panel of viruses was intranasally inoculated into mice at a dose of 2×10^5 PFU. Daily weights of infected mice were obtained (Fig. 2) as an indicator of clinical disease, and lungs were collected to measure viral replication (Fig. 3) and observe histopathology (Fig. 4 and 5).

Unsurprisingly, rNY312 induced little clinical disease, as judged by peak percent weight loss (0.62%). The unadapted avian origin S09RNP virus also caused a low burden of disease, as judged by weight loss (Fig. 2). Consistent with previous studies, viruses containing the RNPs of 1918 and the HPAI H5N1 virus VN1203 (Fig. 2) caused the greatest clinical disease. The peak percent

weight loss of mice infected with 1918RNP (15.9%) was significantly greater than those of mice infected with NY312 ($P < 0.0001$). Forty percent mortality was observed in mice inoculated with VN1203RNP, while no mortality was observed in any other experimental group. Introducing the avian-like PB2-K627E change into the 1918RNP virus rendered the weight loss curve similar to that observed for rNY312 (Fig. 2), while the introduction of the human-like PB2-E627K change into the S09RNP virus increased weight loss somewhat, albeit not significantly (4.93% versus 8.06%; $P = 0.10$). CA09RNP-infected mice lost slightly more weight than those infected with rNY312, but the difference was not statistically significant (4.18% versus 0.62%; $P = 0.23$). Compared to wild-type CA09RNP, CA09RNP-E627K and CA09RNP-D701N induced similarly mild weight losses.

The replicative capacity of these viruses in mouse lung tissue was assessed by titration of lung homogenate from 3, 5, and 7 days postinoculation (dpi). The rescued wild-type human seasonal H1N1 virus, rNY312, grew to a peak titer of 2.6×10^3 PFU/g at 3 dpi. Significantly higher peak titers were achieved by both VN1203RNP (4.2×10^5 PFU/g; $P = 0.0055$) and 1918RNP (7.73×10^5 PFU/g; $P = 0.023$) (Fig. 3). As expected, mutations at PB2-627 significantly affected viral replication in mouse lung tissue.

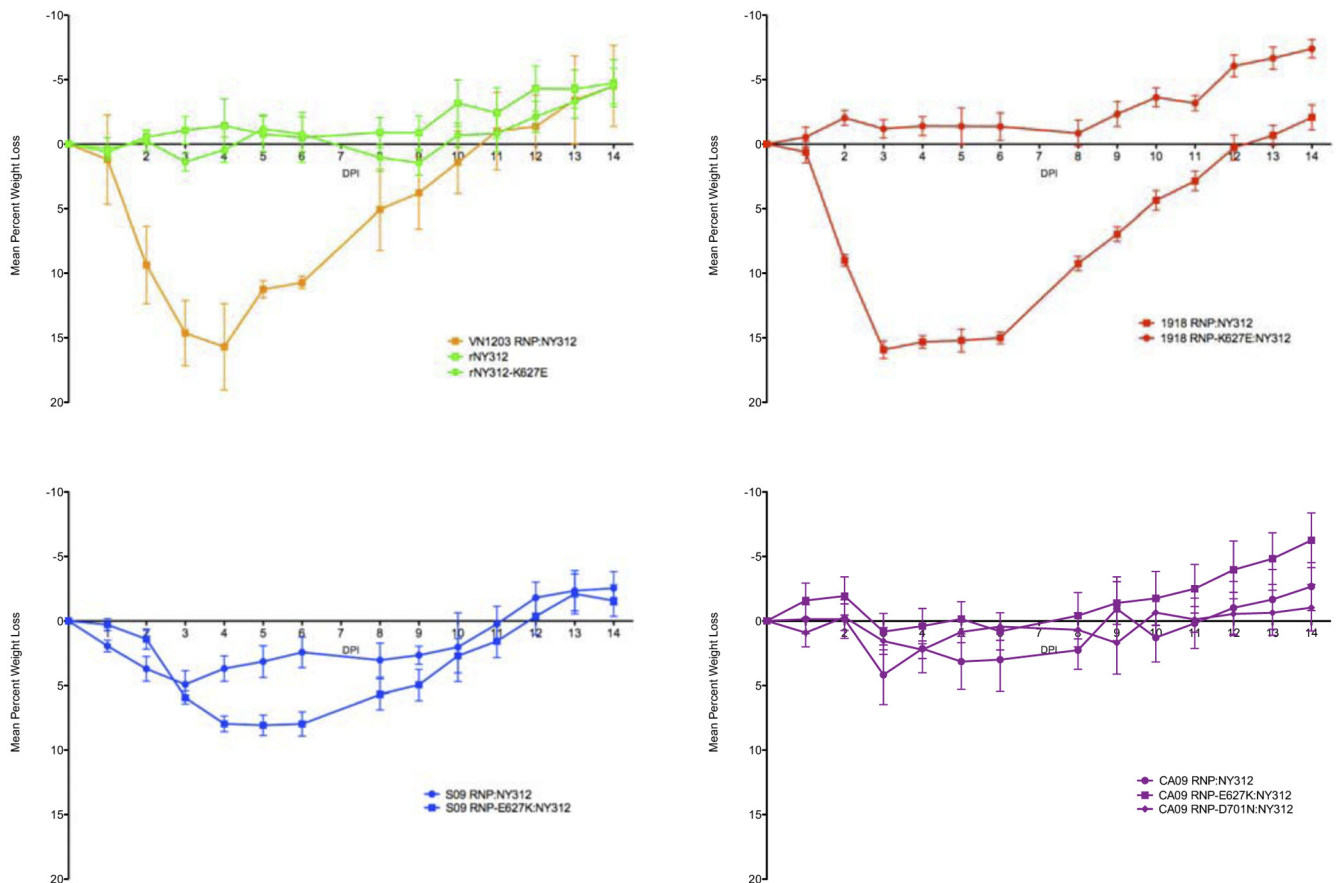


FIG 2 Clinical course of infection in mice as measured by weight loss. Mean percentage body weight loss from mean baseline weight of mice in each group inoculated with rescued A/New York/312/2001 (H1N1) (referred to as rNY312) or chimeric viruses containing the four RNP gene segments of different influenza viruses on the NY312 background (see key) from 0 to 14 days postinoculation (dpi). Groups of five 8- to 10-week-old female BALB/c mice were inoculated intranasally with 2×10^5 PFU of virus. Error bars represent SEM.

Compared to wild-type S09RNP, the S09RNP-E627K virus replicated to approximately 1.5-log-greater titers on day 3 (9.9×10^5

versus 5.2×10^4 PFU/g; $P = 0.025$) and 3-log-greater titers on day 5 (2.27×10^5 versus 1.4×10^2 PFU/g; $P = 0.023$) (Fig. 3). Conversely, 1918RNP-K627E virus replication in mouse lung on day 3 was attenuated by more than 1 log compared to the wild-type 1918 RNP-containing virus (7.73×10^5 versus 4.41×10^4 PFU/g; $P = 0.019$) (Fig. 3) but by day 5 was within 0.5 log of the level for wild-type 1918 RNP (6.53×10^5 versus 2.6×10^5 PFU/g; $P = 0.21$). No virus was detected in any lung on day 7.

The CA09RNP virus also grew to significantly higher peak titers than rNY312 (2.21×10^5 versus 2.6×10^3 PFU/g; $P = 0.043$), confirming the replication competence of this chimeric virus *in vivo*. Again, to our surprise, introduction of the mammalian-adaptive PB2-E627K or -D701N mutation into the pandemic RNP significantly attenuated viral replication in mouse lung. CA09RNP-E627K and CA09RNP-D701N reached approximately 2- and 1-log-lower peak titers than the wild-type CA09RNP virus, respectively (1.1×10^3 and 1.24×10^4 PFU/g versus 2.21×10^5 PFU/g; $P = 0.042$ and 0.049) (Fig. 3).

The histopathology and viral antigen distribution of infected mouse lung tissue were also characterized by analyzing formalin-fixed, stained sections. Consistent with rNY312's mild clinical illness and relatively low lung replication levels, rNY312-inoculated lungs were predominantly within normal limits (Fig. 4), demonstrating only mild focal changes and very rare viral antigen stain-

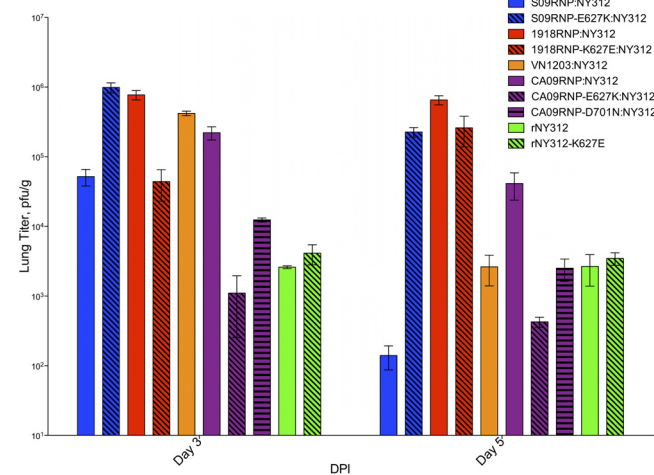


FIG 3 Viral titer in mouse lung tissues. Mean viral titer in mouse lung on days 3 and 5 postinfection was determined by a plaque assay. Data were collected from three mice in each group. Titers are expressed as numbers of PFU per gram of lung tissue. Error bars represent SEM. See the key for the different viruses evaluated.

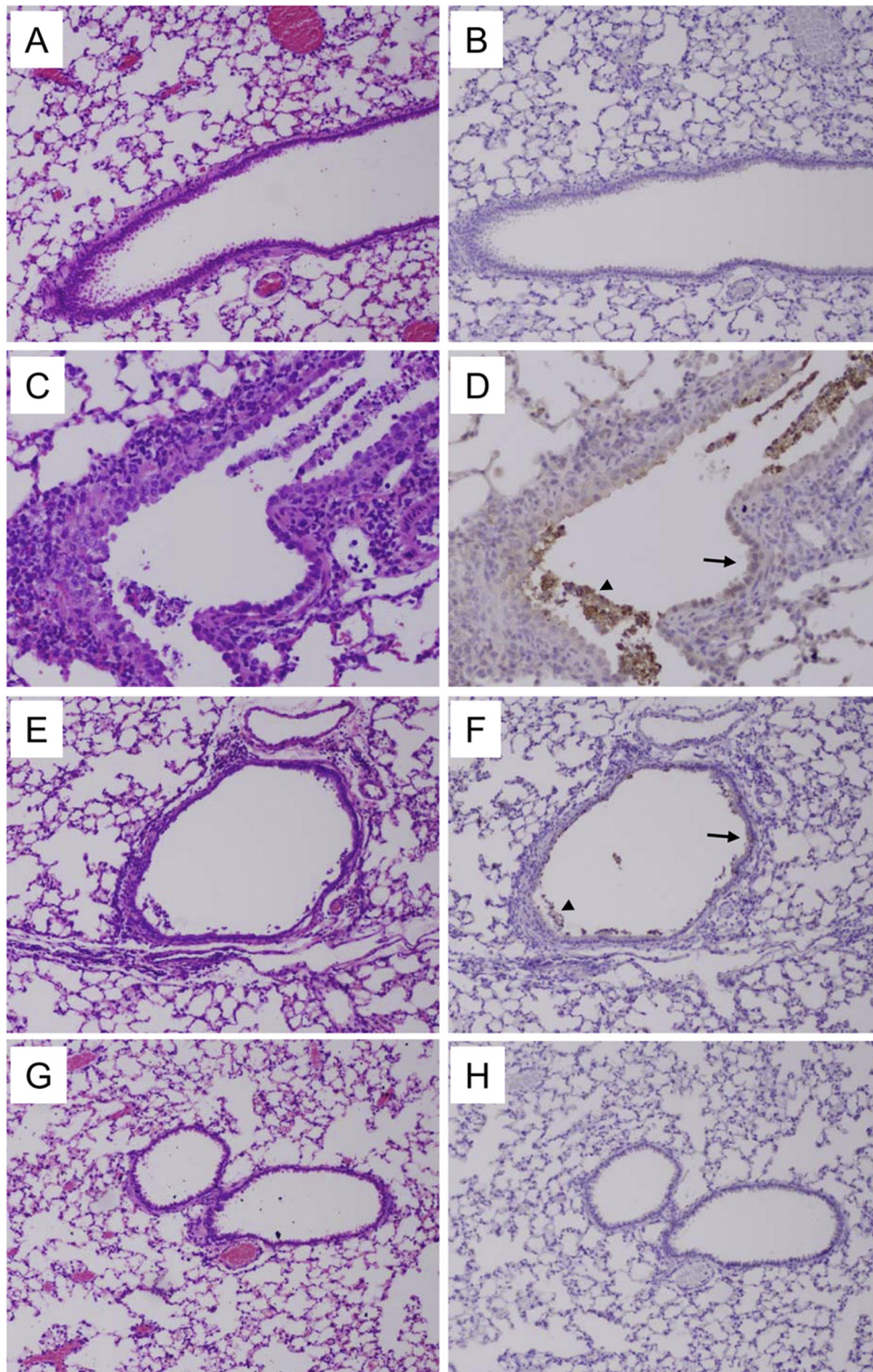


FIG 4 Pathology and immunohistochemistry of influenza virus-infected mouse lung tissue. Photomicrographs of hematoxylin-and-eosin-stained tissue sections and immunohistochemically stained sections for detection of influenza viral antigen from mice infected with different influenza virus constructs at day 5 postinfection. Viral antigen is stained reddish brown on a hematoxylin-stained background. Arrows and arrowheads show examples of positive cells. (A, B) Sections from an animal infected with the rNY312 virus showing no pathological changes in the lung and no viral antigen (original magnifications, $\times 100$). (C, D) Sections from an animal infected with the 1918RNP virus showing marked necrotizing bronchiolitis with a marked transmurular inflammatory cell infiltrate. Prominent viral antigen staining was observed in bronchiolar epithelial cells (arrow) and in necrotic intraluminal debris (arrowhead) (original magnifications, $\times 200$). (E, F) Sections from an animal infected with the CA09RNP virus showing focal bronchiolitis with a minimal inflammatory cell infiltrate. Viral antigen staining was observed in bronchiolar epithelial cells (arrow) and in necrotic intraluminal debris (arrowhead) (original magnifications, $\times 100$). (G, H) Sections from an animal infected with the CA09RNP-E627K virus showing no pathological changes in the lung and no viral antigen (original magnifications, $\times 100$).

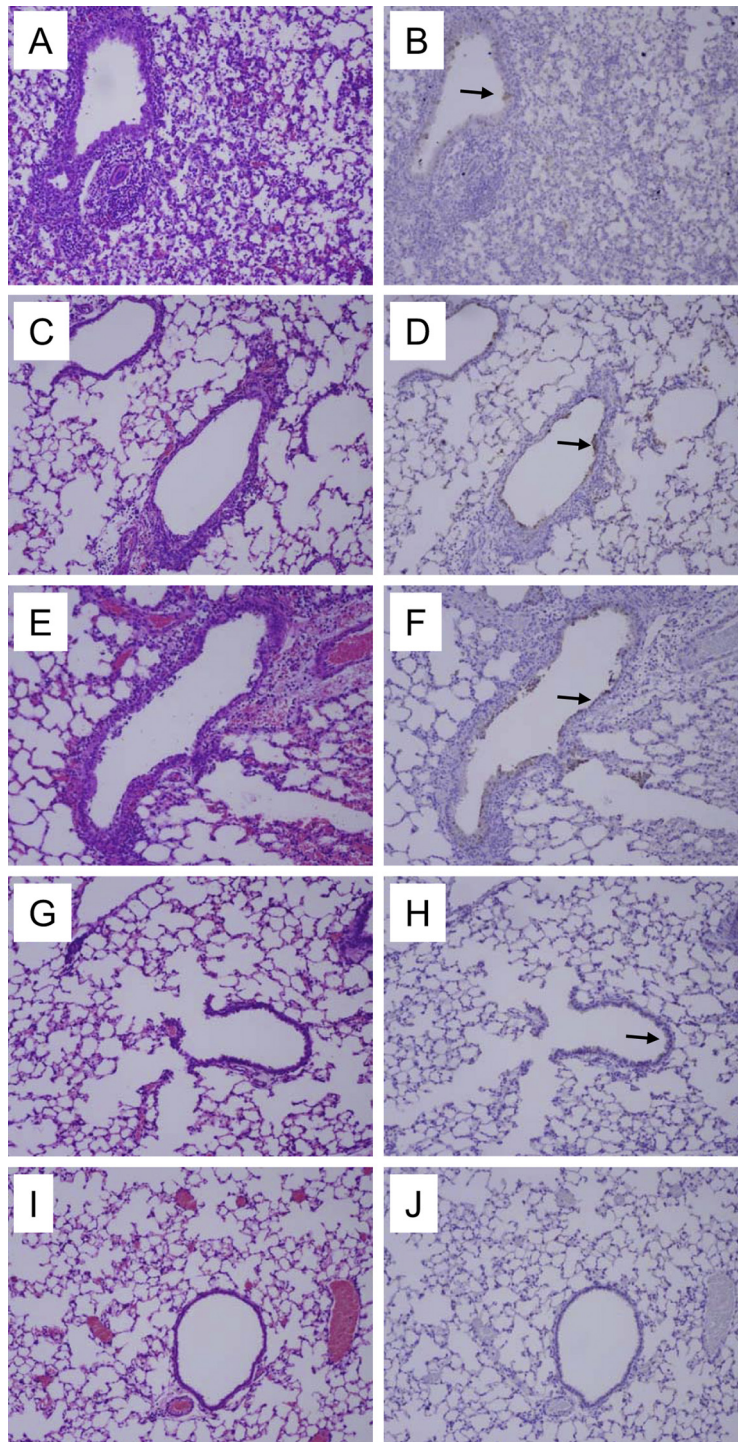


FIG 5 Pathology and immunohistochemistry of influenza virus-infected mouse lung tissue. Photomicrographs of hematoxylin-and-eosin-stained tissue sections and immunohistochemically stained sections for detection of influenza viral antigen from mice infected with different influenza virus constructs at day 5 postinfection (except for the VN1203RNP virus, which is shown at day 3 postinfection). Viral antigen is stained reddish brown on a hematoxylin-stained background. Arrows show examples of positive cells. (A, B) Sections from an animal infected with the S09RNP virus showing a focus of moderate alveolitis. Focal viral antigen is seen in bronchiolar epithelial cells (arrow) and in alveolar macrophages (original magnifications, $\times 100$). (C, D) Sections from an animal infected with the S09RNP-E627K virus showing necrotizing bronchiolitis with a transmural inflammatory cell infiltrate. Viral antigen staining was observed in bronchiolar epithelial cells (arrow) and in alveolar macrophages (original magnifications, $\times 100$). (E, F) Sections from an animal infected with the VN1203RNP virus at day 3 postinfection showing marked necrotizing bronchiolitis with a marked transmural inflammatory cell infiltrate. Prominent viral antigen staining was observed in bronchiolar epithelial cells (arrow) (original magnifications, $\times 100$). Similar histopathological changes were observed at day 5, but only limited viral antigen staining was observed (data not shown). (G, H) Sections from an animal infected with the 1918RNP-K627E virus showing no pathological changes in the lung but some viral antigen staining in bronchiolar epithelial cells (arrow) in the absence of inflammation (original magnifications, $\times 100$). (I, J) Sections from an animal infected with the CA09RNP-D701N virus showing no pathological changes in the lung and no viral antigen (original magnification, $\times 100$).

ing. In contrast, and consistent with previous studies, 1918RNP- and VN1203RNP-inoculated mouse lungs exhibited a pattern of moderate-to-marked necrotizing bronchiolitis with prominent peribronchiolar infiltrates and abundant bronchiolar viral antigen staining (Fig. 4 and 5). As with *in vivo* viral replication, mutations at PB2-627 resulted in significantly different histopathological patterns. The 1918RNP-K627E virus, for example, induced almost no inflammatory changes, resembling the findings seen with rNY312. Introduction of the PB2-E627K change into the low-pathogenicity avian S09RNP virus also altered histopathology. Whereas the wild-type S09RNP virus gave rise to a focal alveolitis with viral antigen in alveolar epithelial cells, the S09RNP-E627K virus instead induced a mild bronchiolitis with increased levels of bronchiolar antigen staining and no alveolitis (Fig. 5).

The CA09RNP virus induced a focal bronchiolitis with a minimal inflammatory infiltrate in infected animals and a predominantly bronchiolar pattern of moderate viral antigen staining (Fig. 4). The introduction of either PB2-E627K or -D701N diminished these findings, resulting in a histopathological picture that was predominantly within normal limits, displaying only rare, focal inflammation (Fig. 4 and 5). Viral antigen staining was rare in lungs infected with either mutant virus.

DISCUSSION

The 2009 H1N1 swine-origin pandemic virus has thus far been relatively mild in its clinical severity, but the fact that it continues to lack certain changes associated with high virulence and host adaptation in other influenza viruses has remained a source for concern. We show that in both A549 cell culture and a mouse model of influenza infection, two of these changes, PB2-E627K and -D701N, do not potentiate the replication or virulence of a virus containing the 2009 pandemic RNP. Rather, both of these changes significantly impair the replication of the virus and diminish the histopathological consequences of infection. Our findings suggest that if the 2009 pandemic virus were to acquire these changes, greater virulence would be an unlikely consequence.

In this study, we have evaluated a series of different RNP gene sets on the same non-RNP background, namely, that of a seasonal human H1N1 virus. Importantly, the wild-type 2009 H1N1 pandemic RNP-containing virus grew to high titers in both cell culture and mouse lung, confirming that the chimeric set of gene segments was compatible and replication competent. Consistent with previous reports, the RNP genes from both the 1918 pandemic virus and a representative HPAI H5N1 lineage virus, VN1203, significantly enhanced pathogenicity. Particularly interesting is the fact that qualitatively different histopathological pictures can be induced with identical HA and NA genes: 1918 and VN1203 RNPs induced a necrotizing bronchiolitis, whereas the parental rNY312 virus did not. In the case of the 1918 RNP, this property proved to be dependent on the presence of PB2-627K, as the 627E mutant virus produced very little clinical or histopathological disease, despite replicating to relatively high titers. In yet another context, that of the avian S09 RNP, the PB2-E627K mutation changed the dominant histopathology from an alveolitis to a bronchiolitis, while the identical mutation was detrimental to pathogenicity in the setting of the CA09 RNP. Thus, the impact of the PB2-627 genotype is at least partly a product of the surrounding ribonucleoprotein genetic context.

A recently published study likewise demonstrated neither any potentiation of viral replication or pathogenicity in 2009 H1N1

pandemic viruses due to PB2-E627K or -D701N in mice or ferrets nor any potentiation of transmission in ferrets (35). Thus, while it is unexpected that the PB2-E627K and -D701N mutations, shown to be beneficial to viral replication in mammalian models in other contexts, attenuate viruses containing the 2009 H1N1 pandemic RNP, it is becoming clear that viral RNP adaptation to humans can be achieved through routes other than PB2-627K or -701N. Indeed, Mehle and Doudna have recently proposed such a residue 627-independent strategy, the so-called “SR” polymorphism, involving residues 590 and 591 (36). It is hypothesized that both strategies may operate by preserving a large positively charged surface domain, implying that this region is involved in interactions with undetermined host-specific factors. Interestingly, when Mehle and Doudna introduced the SR mutations alongside E627K in the avian S09 RNP background, no detriment to viral replication was observed in tissue culture, in contrast to the impaired replication that we observed for viruses containing the 2009 H1N1 RNP. Structural modeling of the 2009 H1N1 PB2 protein may shed light on the underlying mechanism for these findings. Likewise, further biochemical characterization of wild-type and mutant IAV polymerases in different host cell environments may help elucidate the viral processes that are optimized via host adaptive changes.

Thus, the present findings are consistent with our evolving understanding of host switch events in influenza, i.e., that the formation of pandemic influenza viruses, or the emergence of novel swine influenza virus lineages, are independent polygenic processes (37). Evolutionary analyses have demonstrated little evidence of either parallel or convergent mutations in such events, suggesting a strong role for historical contingency in the origination of any particular host-switch genotype (30). Instead, mutations identified as important in one host switch event may or may not be observed in other such events, depending on the viral and host genetic context of each event (30).

While the PB2-E627K mutation clearly carries great significance, it was insufficient to increase replication of an avian RNP-containing virus in human cell culture. Similarly, the K627E back-mutation in the context of rNY312 did not decrease its replication competence *in vitro* or *in vivo*. Moreover, the status of PB2-627 does not by itself determine the viral replication or histopathological phenotype; rNY312 and 1918RNP both possess a lysine at PB2-627 yet exist at opposite ends of those spectra in the present study. Perhaps most intriguingly, in the case of the virus pair comprising 1918RNP and 1918RNP-K627E, a disconnect is observed between the clinical disease and histopathology and viral replication: 1918RNP-K627E is only mildly attenuated in mouse lung replication compared to 1918RNP, yet the 1918RNP-K627E virus causes no clinical illness and virtually no histopathology. As this represents the first known characterization of the 1918 RNP with this mutation, further investigation of this phenotype is warranted. Overall, we conclude that other virulence and host adaptive factors exist alongside PB2-627 as determinants of both host adaptation and pathogenicity.

Future studies are needed to evaluate whether changes at residue 627 or 701 in PB2 would be associated with enhanced transmissibility of the 2009 pandemic virus in humans, but the pandemic virus is clearly able to be transmitted in humans and in animal model systems (35, 38, 39). This study also leaves open the possibility that the pandemic virus could acquire other, yet-undefined changes that could increase virulence and/or transmis-

sibility. Further investigations into the functional significance of these and other host- and virulence-associated genotypes will therefore be key to understanding and combating this important pathogen.

MATERIALS AND METHODS

Generation of synthetic viruses. Viral genome segments were cloned and viruses were rescued as previously described (15, 40). Primers were synthesized (Eurofins-Operon, Huntsville, AL) and mutations introduced into reverse genetics plasmids using a QuikChange site-directed mutagenesis kit according to the manufacturer's instructions (Stratagene, La Jolla, CA). The presence of the introduced mutations and the identity of rescued viruses were verified by sequencing of segments 1 and 4.

Propagation and titration of viruses. Viruses were passaged 1 to 3 times on MDCK (ATCC) cells in the presence of 1 $\mu\text{g/ml}$ *N*-tosyl-L-phenylalanyl chloromethyl ketone (TPCK)-treated trypsin in Dulbecco's modified Eagle's medium (DMEM). Infectious titers of virus stocks were determined by a plaque assay performed in triplicate according to standard protocols.

A549 viral replication kinetics. Triplicate sets of 80% confluent monolayers of A549 (ATCC) cells were inoculated at a multiplicity of infection of 0.01, washed with sterile phosphate-buffered saline (PBS), and overlaid with Opti-MEM (Invitrogen, Carlsbad, CA) supplemented with bovine serum albumin (0.2%) and 1 $\mu\text{g/ml}$ TPCK-treated trypsin. Cells were incubated at 37°C and supernatants sampled at 12-h intervals through 72 h and every 24 h thereafter until 120 h. Infectious titers of supernatants were determined using a plaque assay. Paired *t* tests were performed using GraphPad QuickCalcs, and graphical analysis was accomplished using GraphPad Prism (GraphPad Software Inc., La Jolla, CA).

BALB/c mouse infection. All animal experiments were performed in an enhanced animal BSL3 laboratory at the National Institutes of Health under the auspices of an NIH Animal Care and Use Committee-approved animal study protocol. Groups of 5 8- to 10-week-old female BALB/c mice (JAX Mice and Services, Bar Harbor, ME) were inoculated intranasally with 2×10^5 PFU of virus in 50 μl DMEM under light isoflurane anesthesia. Each mouse was weighed daily; mice losing 25% or more of their body weight compared with the level observed on the day of inoculation were humanely euthanized. Five mice per virus were euthanized on days 3, 5, and 7 postinoculation and lungs collected; three sets of lungs were frozen for virus titration, and two sets were inflated and fixed in 10% neutral buffered formalin for histopathological analysis. Lung viral titers were determined by weighing and homogenizing whole lungs in a 10% (wt/vol) suspension of L15 medium and titrating the homogenate using a plaque assay.

Histopathological analysis. Formalin-fixed mouse lungs were dehydrated and embedded in paraffin and 5- μm sections cut and applied to positively charged slides (American HistoLabs, Gaithersburg, MD). The sections were stained with hematoxylin and eosin and evaluated by a single blinded pathologist. For immunohistochemical staining, antigen retrieval was accomplished in a 10 mM sodium citrate-0.05% Tween 20 buffer using a 2100 Retriever model pressure cooker according to the manufacturer's instructions (Pickcell Laboratories, Amsterdam, Netherlands). The primary antibody was a goat polyclonal anti-influenza A virus IgG (Abcam, Inc., Cambridge, MA), while the secondary antibody was a biotinylated anti-goat IgG (Vectastain elite ABC kit; Vector Laboratories, Burlingame, CA). A 3,3'-diaminobenzidine (DAB) chromogen was used, and the slides were counterstained using hematoxylin.

ACKNOWLEDGMENTS

This work was supported by the Intramural Research Program of the NIH and the NIAID. Authors B.W.J., P.D., and J.K.T. further acknowledge the support of the NIH-Oxford/Cambridge Research Scholars program.

We thank Brian Murphy (NIH/NIAID) for helpful discussions. We

also thank the Comparative Medicine Branch (NIH/NIAID) for assistance with animal studies.

REFERENCES

1. Wright, P. F., G. Neumann, and Y. Kawaoka. 2007. Orthomyxoviruses, p. 1691–1740. In D. M. Knipe and P. M. Howley (ed.), *Fields virology*, 5th ed., vol. 2. Lippincott Williams & Wilkins, Philadelphia, PA.
2. Garten, R. J., C. T. Davis, C. A. Russell, B. Shu, S. Lindstrom, A. Balish, W. M. Sessions, X. Xu, E. Skepner, V. Deyde, M. Okomo-Adhiambo, L. Gubareva, J. Barnes, C. B. Smith, S. L. Emery, M. J. Hillman, P. Rivaller, J. Smagala, M. de Graaf, D. F. Burke, R. A. Fouchier, C. Pappas, C. M. Alpuche-Aranda, H. Lopez-Gatell, H. Olivera, I. Lopez, C. A. Myers, D. Faix, P. J. Blair, C. Yu, K. M. Keene, P. D. Dotson, Jr., D. Boxrud, A. R. Sambol, S. H. Abid, K. St. George, T. Bannerman, A. L. Moore, D. J. Stringer, P. Blevins, G. J. Demmler-Harrison, M. Ginsberg, P. Kriner, S. Waterman, S. Smole, H. F. Guevara, E. A. Belongia, P. A. Clark, S. T. Beatrice, R. Donis, J. Katz, L. Finelli, C. B. Bridges, M. Shaw, D. B. Jernigan, T. M. Uyeki, D. J. Smith, A. I. Klimov, and N. J. Cox. 2009. Antigenic and genetic characteristics of swine-origin 2009 A(H1N1) influenza viruses circulating in humans. *Science* 325: 197–201.
3. Dawood, F. S., S. Jain, L. Finelli, M. W. Shaw, S. Lindstrom, R. J. Garten, L. V. Gubareva, X. Xu, C. B. Bridges, and T. M. Uyeki. 2009. Emergence of a novel swine-origin influenza A (H1N1) virus in humans. *N. Engl. J. Med.* 360:2605–2615.
4. WHO. 11 June 2009, posting date. World now at the start of 2009 influenza pandemic. WHO, Geneva, Switzerland.
5. Morens, D. M., J. K. Taubenberger, and A. S. Fauci. 2009. The persistent legacy of the 1918 influenza virus. *N. Engl. J. Med.* 361:225–229.
6. WHO. 26 February 2010, posting date. Pandemic (H1N1) 2009—update 89. WHO, Geneva, Switzerland.
7. Johnson, N. P., and J. Mueller. 2002. Updating the accounts: global mortality of the 1918–1920 “Spanish” influenza pandemic. *Bull. Hist. Med.* 76:105–115.
8. Barry, J. M., C. Viboud, and L. Simonsen. 2008. Cross-protection between successive waves of the 1918–1919 influenza pandemic: epidemiological evidence from US Army camps and from Britain. *J. Infect. Dis.* 198:1427–1434.
9. Morens, D. M., and J. K. Taubenberger. 2009. Understanding influenza backward. *JAMA* 302:679–680.
10. Reid, A. H., and J. K. Taubenberger. 1999. The 1918 flu and other influenza pandemics: “over there” and back again. *Lab. Invest.* 79:95–101.
11. Taubenberger, J. K., and D. M. Morens. 2006. 1918. Influenza: the mother of all pandemics. *Emerg. Infect. Dis.* 12:15–22.
12. Kobasa, D., A. Takada, K. Shinya, M. Hatta, P. Halfmann, S. Theriault, H. Suzuki, H. Nishimura, K. Mitamura, N. Sugaya, T. Usui, T. Murata, Y. Maeda, S. Watanabe, M. Suresh, T. Suzuki, Y. Suzuki, H. Feldmann, and Y. Kawaoka. 2004. Enhanced virulence of influenza A viruses with the haemagglutinin of the 1918 pandemic virus. *Nature* 431:703–707.
13. Kash, J. C., T. M. Tumpey, S. C. Proll, V. Carter, O. Perwitasari, M. J. Thomas, C. F. Basler, P. Palese, J. K. Taubenberger, A. Garcia-Sastre, D. E. Swayne, and M. G. Katze. 2006. Genomic analysis of increased host immune and cell death responses induced by 1918 influenza virus. *Nature* 443:578–581.
14. Pappas, C., P. V. Aguilar, C. F. Basler, A. Solorzano, H. Zeng, L. A. Perrone, P. Palese, A. Garcia-Sastre, J. M. Katz, and T. M. Tumpey. 2008. Single gene reassortants identify a critical role for PB1, HA, and NA in the high virulence of the 1918 pandemic influenza virus. *Proc. Natl. Acad. Sci. U. S. A.* 105:3064–3069.
15. Qi, L., J. C. Kash, V. G. Dugan, R. Wang, G. Jin, R. E. Cunningham, and J. K. Taubenberger. 2009. Role of sialic acid binding specificity of the 1918 influenza virus hemagglutinin protein in virulence and pathogenesis for mice. *J. Virol.* 83:3754–3761.
16. Watanabe, T., S. Watanabe, K. Shinya, J. H. Kim, M. Hatta, and Y. Kawaoka. 2009. Viral RNA polymerase complex promotes optimal growth of 1918 virus in the lower respiratory tract of ferrets. *Proc. Natl. Acad. Sci. U. S. A.* 106:588–592.
17. WHO. 17 February 2010, posting date. Cumulative number of confirmed human cases of avian influenza A/(H5N1) reported to WHO. WHO, Geneva, Switzerland.
18. Taubenberger, J. K., A. H. Reid, R. M. Lourens, R. Wang, G. Jin, and

- T. G. Fanning. 2005. Characterization of the 1918 influenza virus polymerase genes. *Nature* 437:889–893.
19. Finkelstein, D. B., S. Mukatira, P. K. Mehta, J. C. Obenauer, X. Su, R. G. Webster, and C. W. Naeve. 2007. Persistent host markers in pandemic and H5N1 influenza viruses. *J. Virol.* 81:10292–10299.
 20. Almond, J. W. 1977. A single gene determines the host range of influenza virus. *Nature* 270:617–618.
 21. Subbarao, E. K., W. London, and B. R. Murphy. 1993. A single amino acid in the PB2 gene of influenza A virus is a determinant of host range. *J. Virol.* 67:1761–1764.
 22. Hatta, M., P. Gao, P. Halfmann, and Y. Kawaoka. 2001. Molecular basis for high virulence of Hong Kong H5N1 influenza A viruses. *Science* 293:1840–1842.
 23. Shinya, K., S. Hamm, M. Hatta, H. Ito, T. Ito, and Y. Kawaoka. 2004. PB2 amino acid at position 627 affects replicative efficiency, but not cell tropism, of Hong Kong H5N1 influenza A viruses in mice. *Virology* 320:258–266.
 24. Tarendeau, F., J. Boudet, D. Guilligay, P. J. Mas, C. M. Bougault, S. Boulo, F. Baudin, R. W. Ruigrok, N. Daigle, J. Ellenberg, S. Cusack, J. P. Simorre, and D. J. Hart. 2007. Structure and nuclear import function of the C-terminal domain of influenza virus polymerase PB2 subunit. *Nat. Struct. Mol. Biol.* 14:229–233.
 25. Gabriel, G., A. Herwig, and H. D. Klenk. 2008. Interaction of polymerase subunit PB2 and NP with importin alpha1 is a determinant of host range of influenza A virus. *PLoS Pathog.* 4:e11.
 26. Gabriel, G., B. Dauber, T. Wolff, O. Planz, H. D. Klenk, and J. Stech. 2005. The viral polymerase mediates adaptation of an avian influenza virus to a mammalian host. *Proc. Natl. Acad. Sci. U. S. A.* 102:18590–18595.
 27. Li, Z., H. Chen, P. Jiao, G. Deng, G. Tian, Y. Li, E. Hoffmann, R. G. Webster, Y. Matsuoka, and K. Yu. 2005. Molecular basis of replication of duck H5N1 influenza viruses in a mammalian mouse model. *J. Virol.* 79:12058–12064.
 28. Le, Q. M., Y. Sakai-Tagawa, M. Ozawa, M. Ito, and Y. Kawaoka. 2009. Selection of H5N1 influenza virus PB2 during replication in humans. *J. Virol.* 83:5278–5281.
 29. Steel, J., A. C. Lowen, S. Mubareka, and P. Palese. 2009. Transmission of influenza virus in a mammalian host is increased by PB2 amino acids 627K or 627E/701N. *PLoS Pathog.* 5:e1000252.
 30. Dunham, E. J., V. G. Dugan, E. K. Kaser, S. E. Perkins, I. H. Brown, E. C. Holmes, and J. K. Taubenberger. 2009. Different evolutionary trajectories of European avian-like and classical swine H1N1 influenza A viruses. *J. Virol.* 83:5485–5494.
 31. Salomon, R., J. Franks, E. A. Govorkova, N. A. Ilyushina, H. L. Yen, D. J. Hulse-Post, J. Humberd, M. Trichet, J. E. Rehg, R. J. Webby, R. G. Webster, and E. Hoffmann. 2006. The polymerase complex genes contribute to the high virulence of the human H5N1 influenza virus isolate A/Vietnam/1203/04. *J. Exp. Med.* 203:689–697.
 32. Guan, Y., L. L. Poon, C. Y. Cheung, T. M. Ellis, W. Lim, A. S. Lipatov, K. H. Chan, K. M. Sturm-Ramirez, C. L. Cheung, Y. H. Leung, K. Y. Yuen, R. G. Webster, and J. S. Peiris. 2004. H5N1 influenza: a protean pandemic threat. *Proc. Natl. Acad. Sci. U. S. A.* 101:8156–8161.
 33. Itoh, Y., K. Shinya, M. Kiso, T. Watanabe, Y. Sakoda, M. Hatta, Y. Muramoto, D. Tamura, Y. Sakai-Tagawa, T. Noda, S. Sakabe, M. Imai, Y. Hatta, S. Watanabe, C. Li, S. Yamada, K. Fujii, S. Murakami, H. Imai, S. Kakugawa, M. Ito, R. Takano, K. Iwatsuki-Horimoto, M. Shimajima, T. Horimoto, H. Goto, K. Takahashi, A. Makino, H. Ishigaki, M. Nakayama, M. Okamatsu, K. Takahashi, D. Warshauer, P. A. Shult, R. Saito, H. Suzuki, Y. Furuta, M. Yamashita, K. Mitamura, K. Nakano, M. Nakamura, R. Brockman-Schneider, H. Mitamura, M. Yamazaki, N. Sugaya, M. Suresh, M. Ozawa, G. Neumann, J. Gern, H. Kida, K. Ogasawara, and Y. Kawaoka. 2009. In vitro and in vivo characterization of new swine-origin H1N1 influenza viruses. *Nature* 460:1021–1025.
 34. Koopmans, M. 28 September 2009, posting date. Influenza pandemic (H1N1) 2009 (58): the Netherlands, PB2 mutation. International Society for Infectious Diseases, Brookline, MA.
 35. Herfst, S., S. Chutinimitkul, J. Ye, E. de Wit, V. J. Munster, E. J. Schrauwen, T. M. Bestebroer, M. Jonges, A. Meijer, M. Koopmans, G. F. Rimmelzwaan, A. D. Osterhaus, D. R. Perez, and R. A. Fouchier. 2010. Introduction of virulence markers in PB2 of pandemic swine-origin influenza virus does not result in enhanced virulence or transmission. *J. Virol.* 84:3752–3758.
 36. Mehle, A., and J. A. Doudna. 2009. Adaptive strategies of the influenza virus polymerase for replication in humans. *Proc. Natl. Acad. Sci. U. S. A.* 106:21312–21316.
 37. Taubenberger, J. K., and D. M. Morens. 2009. Pandemic influenza—including a risk assessment of H5N1. *Rev. Sci. Tech.* 28:187–202.
 38. Maines, T. R., A. Jayaraman, J. A. Belser, D. A. Wadford, C. Pappas, H. Zeng, K. M. Gustin, M. B. Pearce, K. Viswanathan, Z. H. Shriver, R. Raman, N. J. Cox, R. Sasisekharan, J. M. Katz, and T. M. Tumpey. 2009. Transmission and pathogenesis of swine-origin 2009 A(H1N1) influenza viruses in ferrets and mice. *Science* 325:484–487.
 39. Munster, V. J., E. de Wit, J. M. van den Brand, S. Herfst, E. J. Schrauwen, T. M. Bestebroer, D. van de Vijver, C. A. Boucher, M. Koopmans, G. F. Rimmelzwaan, T. Kuiken, A. D. Osterhaus, and R. A. Fouchier. 2009. Pathogenesis and transmission of swine-origin 2009 A(H1N1) influenza virus in ferrets. *Science* 325:481–483.
 40. Fodor, E., L. Devenish, O. G. Engelhardt, P. Palese, G. G. Brownlee, and A. Garcia-Sastre. 1999. Rescue of influenza A virus from recombinant DNA. *J. Virol.* 73:9679–9682.